
**AIRCRAFT AND ROCKET
ENGINE THEORY**

Determination of Ingredient Composition of Atmospheric Emissions of the Turbojet Engine Combustion Gases by the Fine-Structure Spectroscopy

N. I. Moskalenko^{*}, R. Sh. Misbakhov^{}, I. Z. Bagautdinov^{***}, N. F. Loktev, and I. R. Dodov**

Kazan State Power Engineering University, ul. Krasnosel'skaya 51, Kazan, 420066 Tatarstan, Russia

**e-mail: NikMoskalenko@list.ru*

***e-mail: zerdex84@mail.ru*

****e-mail: ilyas_81992@mail.ru*

Received April 16, 2015

Abstract—The application of the method of absorbing fine-structure spectroscopy to determine the composition of ingredient emissions of products of combustion of the turbojet engine. Applied for research of ingredient composition of complex spectrophotometric instrumentation provides a measurement of the concentration of the various ingredients in the products of combustion to limit sensitivity of 1–10 ppm. The technology of measurement and processing of the data of spectrometric measurements are discussed. The results of measurements of the ingredient composition released into the atmosphere of the combustion products of the turbojet engine are analysed.

DOI: 10.3103/S106879981603020X

Keywords: spectral transmission function, the spectral line absorption, combustion products, the dispersed phase, ingredient composition.

INTRODUCTION

Ingredient composition of the combustion products is required to meet the challenges in calculating the radioactive heat transfer in power units and determining the efficiency of operation. Combustion products thrown into the atmosphere have ingredients that exert the toxic and carcinogenic effects on flora and fauna. In addition, the strong absorption capacity of man-made emissions have a significant impact on the processes of heat transfer in the Sun–atmosphere–underlying surface system. In recent decades, the optical methods for analyzing the ingredient composition of combustion products have been intensively developed; one of which is a method of fine-structure spectroscopy and spectra radiometry. This method has been successfully used in [1–3] for determining the ingredient composition of combustion products for various fuels on the laboratory measurement systems [3] and in combustion chambers of steam boiler installations. In this paper, we consider the application of the fine-structure spectroscopy method for measuring the ingredient composition of combustion products of turbojet engines.

THE SPECTRAL MEASURING SYSTEM

The spectral measuring system consists of [4–6] a vacuum illuminator, a multi-pass working chamber with internal and external heating, a medium resolution monochromator to measure the absorption spectra in a wide spectral range of 0.3–25 μm , a modernized IKS–21 spectrometer with a set of diffraction gratings operating in the second-order diffraction, and a Girard scanning spectrometer of high spectral resolution $\Delta = 0.05 - 0.1 \text{ cm}^{-1}$. Harmonization of various modules of the spectral measuring system is

performed by means of optical attachments. A measuring system was used to record both the spectra of radiation attenuation of the medium being studied in the working chamber and the radiation of the medium in order to identify an opportunity for remote diagnostics of aerocarrier traces by their thermal radiation [5, 7]. The measurements performed have shown that the absorbance spectra of the environment coincides with the spectrum emissivity of the medium within the measurement error that does not exceed 2–3 % in gases at temperatures of 300–900 K. Figure 1 presents an example of the spectrograms recorded for CO over the range 2148–2167 cm^{-1} with the resolution $\Delta = 0.06 \text{ cm}^{-1}$. Figure 2 presents an example of the spectrograms recorded for HCl in the vicinity of frequencies 2864 and 2842 cm^{-1} with the resolution $\Delta = 0.09 \text{ cm}^{-1}$.

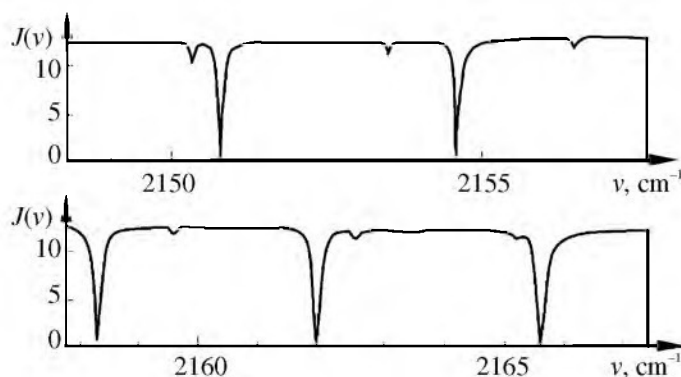


Fig. 1.

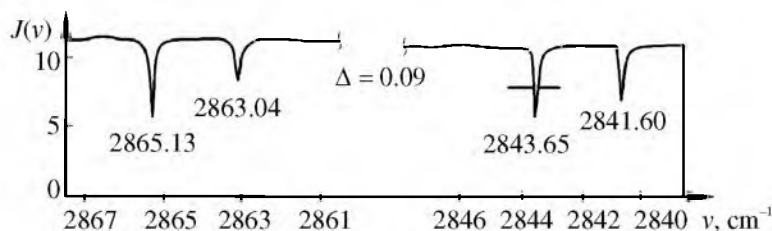


Fig. 2.

METHOD FOR DETERMINING THE CONCENTRATION OF INGREDIENTS FROM THE ABSORPTION SPECTRA OF HIGH RESOLUTION

The spectral transmittance function (STF) is determined from the spectrograms $J(v)$ measured according to the formula $\tau(v) = J(v)/J_0(v)$, where $J_0(v)$ is the base line. In the spectrum regions, where the spectral lines are absent (transparency windows), the STF is determined only by the radiation attenuation of the dispersed phase and the volume concentration of volatile sol is determined from the values $\tau(v)$ in the transparency windows. For the instrumental function of the spectrometer δ_v we have

$$\tau_{\delta_v} = \tau_{\delta_v}^0 / \tau_a(v),$$

where $\tau_{\delta_v}^0$ is the STF based on molecular absorption and radiation attenuation by an aerosol. For the multicomponent medium

$$\tau_{\delta_v} = \prod_i \tau_{\delta_v}^i,$$

where $\tau_{i\delta_\nu}$ is the STF for the i th component of the gas phase. In the case of high spectral resolution, let us decompose the function $A_{\delta_\nu} = |\ln \tau_{\delta_\nu}|$ into separate components using the method of differential moments. To this end, the spectra measured are subjected to partitioning with a step $\delta = \Delta/5$, where Δ is the spectral resolution of the spectrometer. Random noise reduction is attained by a five-point smoothing procedure by a spline in the form of a fifth degree polynomial. The digital spectrum obtained is decomposed into the individual components of lines

$$A(\nu) = \sum_{m=1}^M A_m \left[\sum_{n=1}^N A_{mn} (\nu - \nu_m^0)^n \right]^{-1},$$

where A_m is the maximum intensity of the m th component; A_{mn} are the coefficients of the generalized circuit

$$g_m = \frac{1}{\sum_{n=1}^N A_{mn} (\nu - \nu_m^0)^n}.$$

Characteristics A_{mn} provide the complete information about the individual circuits and are defined as the Taylor series expansion coefficients of a function $f_m(\nu)$ that describes the m th circuit:

$$f_m(\nu) = \frac{1}{m!} \sum_{m=0}^N A_{mn} (\nu - \nu_m^0)^m,$$

where the value A_{mn} is the maximum amplitude of the contour. The centre ν_m^0 is determined from the condition that the coefficient A_{m1} is equal to zero; the half-width value of the m th line is obtained by the following relation

$$\alpha_{L_m} \sqrt{\frac{\sqrt{A_{m2}^2 + 4A_{m4}} - A_{m2}}{2A_{m4}}}.$$

The so-obtained profiles are restored with taking into account the instrumental function of the spectrometer [1, 2].

Thus, we have the separate circuits of the function $A_m(\nu)$ with the centers ν_m^0 that are identified by the ingredients on the basis of a priori information on the centers of their spectral lines. The absorption lines identified are denoted by the sign i that is the ingredient numbers, their centers, contours, half-widths ν_m^{0i} , $K_m^i(\nu)$, α_m^i contain information on the ingredient concentration. Really, for the Lorentz contour $b_m^i(\nu)$ we get

$$K_m^i(\nu) = \frac{A_m^i(\nu)}{\omega_i}, \quad S_m^i = \int K_m^i(\nu) d\nu = K_{\nu m}^i \pi \alpha_m^i,$$

where S_m^i is the intensity of the m th line of the ingredient i ; $K_{\nu m}^i$ is the absorption coefficient at the line center; α_m^i is the half-width of the m th line of the component i ; $\omega_i = \rho_i L$, L is the length of the optical path in the working chamber, ρ_i is the volume concentration of the ingredient i ; $\alpha_m^i = \alpha_{0m}^i P_{eff}^i$; P_{eff}^i is the effective pressure in the working chamber; α_{0m}^i is the half-width at standard pressure

$$P_{eff}^i = P_{iN_2} + \sum_{K=1}^N P_K B_{ik}.$$

In determining the concentration of volatile components in the present study, use is made of the experimental data on the parameters of spectral lines [8–18] that were recalculated for the temperature of the working chamber by the relations presented in [8, 13, 18, 19].

DETERMINATION OF THE MICROSTRUCTURE OF THE DISPERSED PHASE OF THE COMBUSTION PRODUCTS

Determination of the microstructure of the sooty sol in combustion products by the optical method is an inverse problem. Solution of this problem requires a priori information on the optical characteristics of the sooty sol of different microstructure formations spanning the entire area of the spectral variations of radiation attenuation and absorption coefficients. In this case, the reference wavelengths (measurement channels) should be selected in the transparency windows of the gas phase of the combustion products with the minimum contribution to the absorption of radiation in the attenuation spectra being recorded. This spectra should include the wavelengths in the visible, ultraviolet and infrared ranges of spectrum [20].

Optimization of solving the problem of restoring the sol microstructure from the radiation attenuation spectra is carried out with respect to the following condition

$$\sum_i \frac{\Delta\sigma_{a\lambda i}}{\sigma_{a\lambda i}} = \min,$$

where $\Delta\sigma_{a\lambda i}$ are deviations in the spectral dependence of the attenuation coefficient of the restored spectrum $\sigma_{a\lambda i}$ on the measured one; i is the number of measurement channel.

Particles are porous and include a soluble fraction and inclusions of the gas phase in their composition. Measurements have shown that the density of sooty sol depends on the combustion mode [20] and varies within the scope of values $\rho \in \{1, 9; 2, 4\}$ wherein the soluble fraction of the sol is about 10% of the total mass of particles during combustion of gaseous fuel. We calculated the optical performance of the model microstructures of the sooty sol particles for the modified gamma distribution with the modal particle radiuses from 1.6×10^{-3} to $2.25 \mu\text{m}$ in accordance with the given composition of the sooty sol. The electronic database [20] was used to determine the sooty sol microstructure of these spectral optical measurements. At the same time, the microstructure determination is based on the recovery of the aerosol STF $\tau_{a\lambda}$ for the attenuation spectra measured and determination of the spectral dependence $\sigma_{a\lambda}$.

Approach $\sigma_{a\lambda}^0$ is selected according to the relation [9]. Further, the microstructure of the sooty sol is determined, using an iterative solution adjustment procedure by the perturbation method (Tikhonov's descent method) in compliance with the microstructure normalization of each iteration, by the following ratio:

$$\sum_k \ln \tau_{ak}(\lambda = 0.55 \mu\text{m}) = \ln \tau_a(\lambda = 0.55 \mu\text{m}),$$

where k is a number of fractions including the fraction of the zero approximation; τ_a is the STF of aerosol for $\lambda = 0.55 \mu\text{m}$.

The essence of the task of the sol microstructure restoring is that the weight fractions of $N_i(r)$ particles should be determined. These fractions are the best way to describe the spectral dependence of the radiation attenuation and absorption coefficients measured.

DISCUSSION OF RESEARCH RESULTS

Tables 1–3 present the ingredient composition of the gas phase for the combustion products of the R-27V-300, R-25-300, R-9V aircraft jet engines emissions. The main optically active ingredients that determine the radiation heat transfer in the engine and atmospheric aircraft trail are vapors H_2O , CO_2 , CO . A large concentration of CO in the emissions is observed for all engines and in some cases reaches 50% of the CO_2 concentration. Trial is composed of nitrogen oxides NO , NO_2 , N_2O . Volatile and non-volatile hydrocarbons in the atmosphere, as a result of photochemical reactions, are transformed into CH_4 and the sooty sol CO in the presence of NO is also transformed into CH_4 causing the greenhouse effect. Heavy hydrocarbons (alcohols, phenols) are destroyed in oxidation by tropospheric ozone causing a decrease in its concentration. Traces of H_2O_2 , SO_2 , and HCOH are also observed in emissions.

Table 1

| Engine | The volume concentration of ingredient (in percent) | | | | |
|-----------|---|-----------------|------|----------------|----------------|
| | H ₂ O | CO ₂ | CO | N ₂ | O ₂ |
| R-27V-300 | 6.9 | 4.77 | 1.27 | 75.9 | 10.1 |
| R-25-300 | 6.1 | 4.1 | 1.95 | 76.8 | 11.1 |
| R-9-V | 5.3 | 3.1 | 2.2 | 77.3 | 12.1 |

Table 2

| Engine | The volume concentration of ingredient (ppm) | | | | | | | | |
|-----------|--|-----------------|------------------|------|-------------------------------|-------------------------------|-------------------------------|-----------------|--------------------|
| | NO | NO ₂ | N ₂ O | HCOH | C ₂ H ₂ | C ₂ H ₄ | C ₂ H ₆ | CH ₄ | CH ₃ OH |
| P-27V-300 | 80 | 25 | 3 | 20 | 34 | 30 | 10 | 56 | 90 |
| P-25-300 | 75 | 23 | 3 | 25 | 30 | 26 | 12 | 60 | 75 |
| P-9-V | 60 | 20 | 4 | 30 | 30 | 20 | 14 | 46 | 60 |

Table 3

| Engine | The volume concentration of ingredient (ppm) | | | | | | | | | |
|-----------|--|---------------------------------|----------------------------------|-------------------------------|---|---|---------|-----------------|-------------------------------|--------------|
| | C ₂ H ₄ O | C ₄ H ₈ O | C ₆ H ₁₂ O | C ₆ H ₆ | C ₆ H ₅ CH ₂ | C ₆ H ₄ (CH ₃) ₂ | Styrene | SO ₂ | H ₂ O ₂ | Benzaldehyde |
| P-27V-300 | 30 | 15 | 50 | 160 | 100 | 90 | 80 | 4 | 38 | 50 |
| P-25-300 | | 15 | 55 | 150 | 110 | 95 | 90 | 4 | 40 | 56 |
| P-9-V | 25 | 23 | 70 | 120 | 130 | 120 | 110 | 4 | 45 | 80 |

The dispersed phase of aircraft kerosene emissions in the engine is caused by forming the sooty sol as a result of the ion nucleation from the gas phase with the following heterogeneous coagulation. The rate of forming the primary sol depends on the electrical properties of the fuel combustion medium. The experimental data and theoretical consideration of the mechanism of forming the sol shows that the particles with a radius of $r \geq 0.001 \mu\text{m}$ remain in the flames. The most probable particle radius of the primary sol is $r_m = 0.003 \mu\text{m}$ [9, 20, 21]. The further particle growth of the primary sol is caused by heterogeneous coagulation, the efficiency of which depends on the numerical density of particles of the primary sol, their electrical properties as well as the residence time of particles in the engine. The sooty sol microstructure can be described by the following relation

$$\frac{f[r(t)]}{f_0(r)} = \sum_i \left[1 + \frac{1}{2} K_i n_{0i} \ln \left\{ \frac{1 + \alpha_i t}{\alpha_i} \right\} \right]^{\sqrt[3]{}} + \sum_{i \neq k} \left[1 + \frac{1}{2} K_{ik} (n_{0i} n_{0k})^{\sqrt[2]{}} \ln \left\{ \frac{1 + \alpha_{ik} t}{\alpha_{ik}} \right\} \right]^{\sqrt[3]{}},$$

where $f_0(r)$ is the initial distribution of the particle number by dimensions during the fuel combustion; t is the residence time of combustion products in the engine; $f[r(t)]$ is the distribution of particles at the engine nozzle exit; K_i , K_{ik} are the coagulation factors.

The values α_i^{-1} , α_{ik}^{-1} determine the time for which the dimensions of particles i and $i - k$ will doubled. By changing the values $\alpha_i(t)$, $\alpha_{ik}(t)$, $K_i(t)$, $K_{ik}(t)$, we can take into account the effect of heterogeneous and homogeneous coagulation on the temporal variations of the sol microstructure.

Changes in the sol microstructure leads to variations in the spectral dependence of its optical characteristics, namely, the coefficients of radiation absorption, radiation dispersion by particles and dispersion index. The results of processing the spectral coefficients of radiation attenuation by combustion products showed that the sooty sol microstructure can be described as a superposition of three gamma-distributions of the following form

$$f(r_a) = Ar^a \exp[-br^c],$$

where the parameters a , b , c determine the shape of the distribution curve of the particle number by their dimensions. The modal radius is

$$r_m = \left(\frac{a}{bc} \right)^{1/c}.$$

The parameters a , b , c , r_m take the values: 1; 50; 0.5; $1.6 \times 10^{-3} \mu\text{m}$, 0.2; 6; 0.5; $4.4 \times 10^{-3} \mu\text{m}$, 1; 9; 0.5; $4.9 \times 10^{-2} \mu\text{m}$ for three gamma-distributions of the sol microstructure particles, respectively.

Optical characteristics of the sooty sol (normalized absorption and dispersion coefficients, dispersion index) are calculated for these distributions in the spectrum of wavelengths in a spectral range of 0.2–

50 μm . The optical density of the sooty sol $\frac{\partial \tau_a}{\partial L}$ is determined by measurements of the optical thickness at

the wavelength $\lambda = 0.55 \mu\text{m}$ and varies over the range $\frac{\partial \tau_a}{\partial L} \in \{0.03; 0.05\} \text{ m}^{-1}$

REFERENCES

1. Moskalenko, N.I. and Safiullina, Ya.S., Application of the Fine-Structure Spectroscopy for the Determination of Ingredient Composition of the Fuel Combustion Products, *Izv. Vuz. Problemy Energetiki*, 2009, nos. 1–2, pp. 22–32.
2. Moskalenko, N.I., Loktev, N.F., Safiullina, Ya.S., and Sadykova, M.S., Ingredients Identification and Determination of Ingredient Composition of Atmospheric Emissions and Combustion Products by Means of Fine-Structure Spectrometry Method, *Alternativnaya Energetika i Ekologiya*, 2010, no. 2, pp. 43–54.
3. Isaev, A.I., Safarbakov, A.M., and Mairovich, Yu.I., On Choice of a Swirler for the Impulse Combustion Chamber, *Izv. Vuz. Av. Tekhnika*, 2013, vol. 56, no. 4, pp. 63–67 [Russian Aeronautics (Engl. Transl.), vol. 56, no. 4, pp. 407–413].
4. Moskalenko, N.I., Aver'yanova, A.V., Mirumyants, S.O., Zotov, O.V., and Il'in Yu.A., An Apparatus for Multiple Investigations of the Characteristics of the Molecular Absorption of Irradiation by Atmospheric Gases, *Zhurnal Prikladnoi Spektroskopii*, 1973, vol. 19, no. 4, pp. 752–756 [Journal of Applied Spectroscopy (Engl. Transl.), vol. 19, no. 4, pp. 1379–1382].
5. *Tekhnika i tekhnologiya v XXI veke: sovremennoe sostoyanie i perspektivi razvitiya* (Engineering and Technology in the Twenty-First Century: State of the Art and Prospects for Development), Chernova, S.S., Ed., Novosibirsk: TsRNS, 2009, pp. 13–47.
6. Gureev, V.M., Mats, E.B., Ivanova, V.N., Gureev, M.V., Malyshkin, D.A., and Agalakov, Yu.R., Processing Feasibilities of Enhancing the GTE-Based Electric Power Plant Efficiency, *Izv. Vuz. Av. Tekhnika*, 2013, vol. 56, no. 2, pp. 57–60 [Russian Aeronautics (Engl. Transl.), vol. 56, no. 2, pp. 179–184].
7. *Optoelectronics – Devices and Applications*, Predeep, P., Ed., Croatia: InTech, 2011.
8. Kondrat'ev, K.Ya. and Moskalenko, N.I., *Teplovoye izluchenie planet* (Thermal Radiation of Planets), Leningrad: Gidrometeoizdat, 1977.
9. Kondrat'ev, K.Ya., Moskalenko, N.I., and Pozdnyakov, D.V., *Atmosfernyi aerosol* (Atmospheric Aerosol), Leningrad: Gidrometeoizdat, 1983.
10. Moskalenko, N.I. and Mirumyants, S.O., *Atlas spektrov prozrachnosti po proizvol'no orientirovannym trassam atmosfery* (Atlas of Transparency Spectra of Randomly Oriented Routes Atmosphere), Moscow: TsNII i TEI, 1979.
11. Moskalenko, N.I. and Loktev, N.F., Simulation Methods of Selective Radiation Transfer in Structurally Inhomogeneous Media, *Teplovyte Protssesy v Tekhnike*, 2009, vol. 1, no. 10, pp. 432–435.
12. Moskalenko, N.I., Mirumyants, S.O., Loktev, N.F. et al., *Ravnovesnye i neravnovesnye protsessy izlucheniya: vysokie temperatury, radiatsionnyi teploobmen* (Equilibrium and Non-Equilibrium Processes of Radiation: High Temperatures, Radiation Heat Transfer), Kazan: KGEU, 2015.
13. Moskalenko, N.I., Il'in, Yu.A., and Kayumov, G.V., Measuring System with High Spectral Resolution for Investigating Flames, *Zhurnal Prikladnoi Spektroskopii*, 1992, vol. 56, no. 1, pp. 122–127 [Journal of Applied Spectroscopy (Engl. Transl.), vol. 56, no. 1, pp. 93–97].

14. Moskalenko, N.I., Zotov, O.V., and Mirumyants, S.O., Experimental Investigation of the Parameters of the CO₂ Absorption Spectral Lines, *Zhurnal Prikladnoi Spektroskopii*, 1974, vol. 21, no. 5, pp. 893–899 [Journal of Applied Spectroscopy (Engl. Transl.), vol. 21, no. 5, pp. 1532–1537].
15. Moskalenko, N.I., Measuring the Intensity and Half-Width of the Spectral Absorption Lines of the Baseband 0–1 CO, *Optika i Spektroskopiya.*, 1975, vol. 38, no. 4, pp. 676–680.
16. Gortyshov, Yu.F., Gureev, V.M., Misbakhov, R.S. et al., Influence of Fuel Hydrogen Additives on the Characteristics of a Gas-Piston Engine under Changes of an Ignition Advance Angle, *Izv.Vuz. Av. Tekhnika*, 2009, vol. 52, no. 4, pp. 73–74 [Russian Aeronautics (Engl. Transl.), vol. 52, no. 4, pp. 488–490].
17. Kayumova, G.V. and Moskalenko, N.I., Atlases of Spectral Lines Parameters and Radiation Absorption by Atmospheric CO, NO, and HCL, *Tezisy dokladov pyatogo vsesoyuznogo simpoziuma po rasprostraneniyu lazernogo izlucheniya v atmosphere* (Proc. 5th All-Union Symposium on the Propagation of Laser Radiation in the Atmosphere), Tomsk, 1979, pp. 182–186.
18. Rosman, L.S., Gordon, I.E., Barbe, A., Benner, D.C. et al., The HITRAN 2008 Molecular Spectroscopic Database, *Journal of Quantitative Spectroscopy and Radiative Transfer*, 2009, vol. 110, nos. 9–10, pp. 533–572.
19. Tsatiashvili, V.V., Impact of Agents Mixing Velocity in Diffusion Flame on Nitric Oxide Emission, *Izv.Vuz. Av. Tekhnika*, 2013, vol. 56, no. 1, pp. 38–43 [Russian Aeronautics (Engl. Transl.), vol. 56, no. 1, pp. 50–58].
20. Moskalenko, N.I., Safiullin, J.S., and Zagidullin, R.A., Microstructure and Radiation Characteristics of Sooty Ashes Particulates in Flames and Anthropogenic Combustion Products, *Izv. Vuz. Problemy Energetiki*, 2013, nos. 5–6, pp. 23–32.
21. Markushin, A.N., Baklanov, A.V., and Tsyganov, N.E., Improvement of Aircraft GTE Emission Characteristics by Using the Microflame Fuel Combustion in a Shortened Combustion Chamber, *Izv.Vuz. Av. Tekhnika*, 2013, vol. 56, no. 4, pp. 59–62 [Russian Aeronautics (Engl. Transl.), vol. 56, no. 4, pp. 401–406].